

Supplementary Information

Design of Inhibitors That Target the Menin-Mixed Lineage Leukemia Interaction

Moses N. Arthur ^{1,2,†}, Kristeen Bebla ^{3,4,†}, Emmanuel Broni ^{3,†}, Carolyn Ashley ³, Miriam Velazquez ³, Xianin Hua ⁵, Ravi Radhakrishnan ^{6,7,8}, Samuel K. Kwofie ^{9,10,*} and Whelton A. Miller III ^{3,4,7,*}

1 Department of Parasitology, Noguchi Memorial Institute for Medical Research (NMIMR), College of Health Sciences (CHS), University of Ghana, Legon, Accra LG 581, Ghana; marthur3@ur.rochester.edu

2 Biomedical Engineering Department, University of Rochester, Rochester, NY 14627, USA

3 Department of Medicine, Loyola University Medical Center, Loyola University Chicago, Maywood, IL 60153, USA; kbebla@luc.edu (K.B.); ebroni@luc.edu (E.B.); cashley1@luc.edu (C.A.); mvelazquez4@luc.edu (M.V.)

4 Department of Molecular Pharmacology & Neuroscience, Loyola University Medical Center, Loyola University Chicago, Maywood, IL 60153, USA

5 Department of Cancer Biology, Perelman School of Medicine, University of Pennsylvania, Philadelphia, PA 19104, USA; huax@mail.med.upenn.edu

6 Department of Bioengineering, School of Engineering and Applied Science, University of Pennsylvania, Philadelphia, PA 19104, USA; rradhak@seas.upenn.edu

7 Department of Chemical and Biomolecular Engineering, School of Engineering and Applied Science, University of Pennsylvania, Philadelphia, PA 19104, USA

8 Department of Biochemistry and Biophysics, Perelman School of Medicine, University of Pennsylvania, Philadelphia, PA 19104, USA

9 Department of Biomedical Engineering, School of Engineering Sciences, College of Basic & Applied Sciences, University of Ghana, Legon, Accra LG 77, Ghana

10 Department of Biochemistry, Cell and Molecular Biology, West African Centre for Cell Biology of Infectious Pathogens, College of Basic and Applied Sciences, University of Ghana, Accra LG 54, Ghana

* Correspondence: skkwofie@ug.edu.gh (S.K.K.); wmiller6@luc.edu (W.A.M.III)

† These authors contributed equally to this work.

Content

Figure S1: Potential energy plot of menin after energy minimization using OPLS and CHARMM36 force fields.

Figure S2: Root mean squared deviation (RMSD) [(a) and (b)] and Radius of gyration (Rg) [(c) and (d)] plots after 20 ns MD simulation of menin using OPLS and CHARMM36 force fields for: (a) and (c) full protein including disordered regions; and (b) and (d) only structured part.

Figure S3: Superimposition of the best pose from AutoDock Vina docking to the co-crystallized structures for (a) MI-2 (ORO), (b) MI-2-2 (ORT), (c) MI-89, and (d) MIV-6. For all the superimpositions, the co-crystallized ligands are in red while the docking poses are coloured yellow.

Figure S4: Protein-ligand interaction maps of menin in complex with (a) CID 71777742, (b) ZINC000103526876, (c) ZINC000085530497, (d) ZINC000095912718, (e) ZINC000070451048, (f) ZINC000085530488, (g) ZINC000095912706, (h) ZINC000103580868, and (i) ZINC000103584057.

Figure S5: Radius of gyration plots of only the structured region of the unbound menin protein and the menin-ligand complexes generated using GROMACS after 100 ns simulation. The Rg plots were generated using: (a) and (b) whole menin structure from MD run 1; (c) and (d) whole menin structure from MD run 2; (e) and (f) only structured regions of menin from MD run 2; (g) and (h) whole menin structure from MD run 3; and (i) and (j) only structured regions of menin from MD run 3. The unbound protein is coloured black while the known inhibitors CID 71777742, CID 36294 and 0RT are coloured red, green, and blue, respectively.

Figure S6: Root mean square deviation of the unbound menin protein and the menin-ligand complexes generated using GROMACS after 100 ns simulation. The RMSD plots were generated using: (a) and (b) whole menin structure from MD run 1; (c) and (d) whole menin structure from MD run 2; (e) and (f) only structured regions of menin from MD run 2; (g) and (h) whole menin structure from MD run 3; and (i) and (j) only structured regions of menin from MD run 3. The unbound protein is coloured black while the known inhibitors CID 71777742, CID 36294, and 0RT are coloured red, green and blue, respectively.

Figure S7: Root mean square fluctuation plots for menin-ligand complexes generated using GROMACS after 100 ns simulation for (a) MD run 2 and (b) MD run 3. The known inhibitors CID 71777742, CID 36294 and 0RT are coloured as purple, red, and green, respectively.

Figure S8: Per-residue energy decomposition of the menin-ligand complexes: (a) 0RT, (b) 36294, (c) 71777742, (d) ZINC000095912705, (e) ZINC000103526876, (f) ZINC000085530497, (g) ZINC000095912718, (h) ZINC000070451048, (i) ZINC000085530488, (j) ZINC000095912706, (k) ZINC000103580868, and (l) ZINC000103584057.

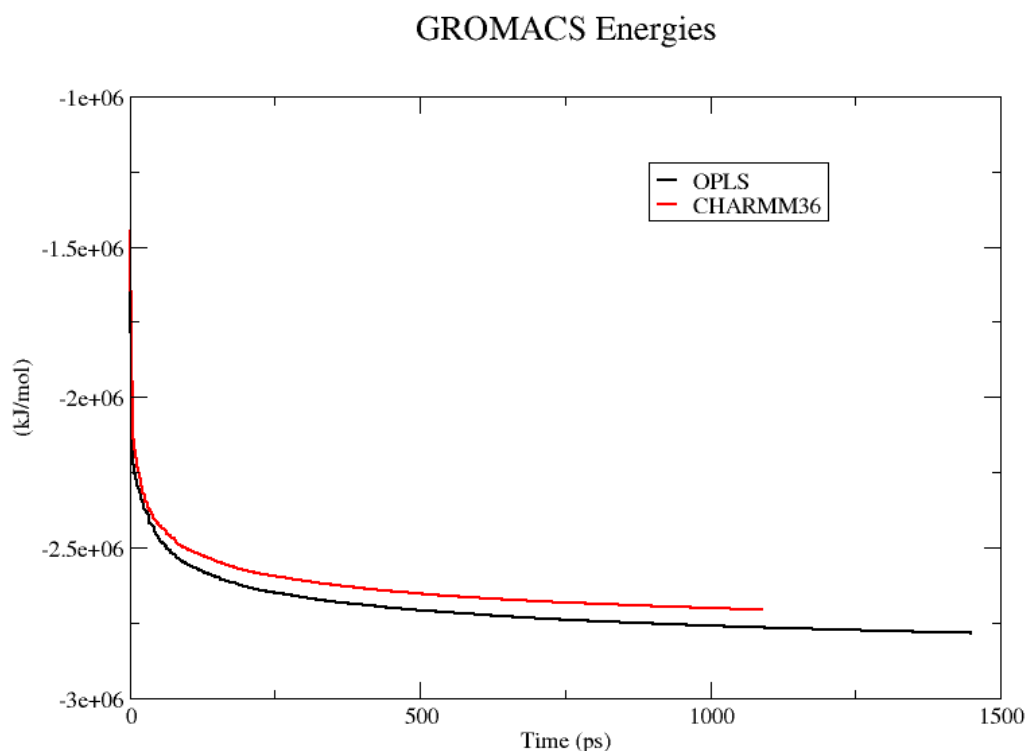


Figure S1. Potential energy plot of menin after energy minimization using OPLS and CHARMM36 force fields.

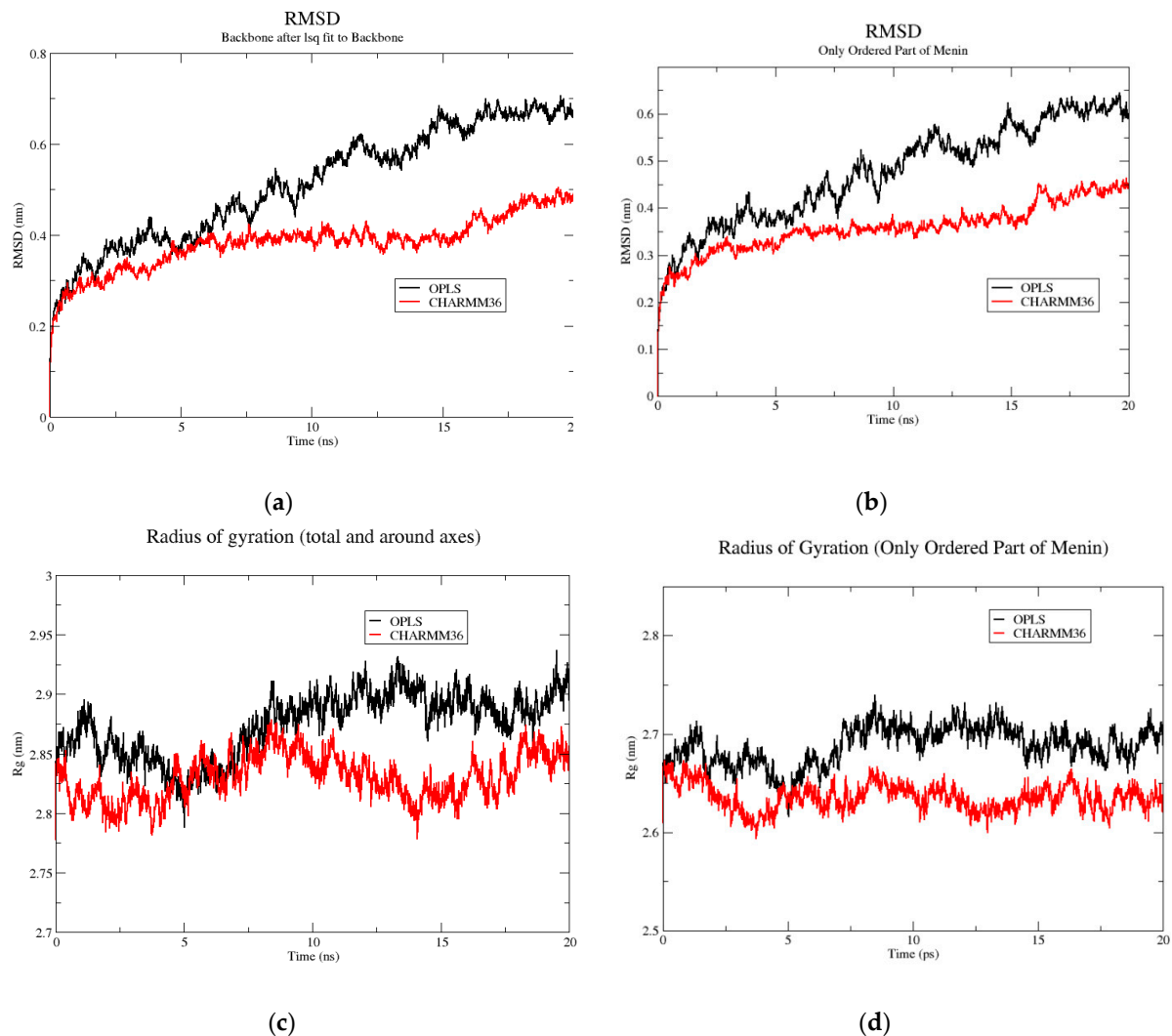


Figure S2. Root mean squared deviation (RMSD) [(a) and (b)] and Radius of gyration (Rg) [(c) and (d)] plots after 20 ns MD simulation of menin using OPLS and CHARMM36 force fields for: (a) and (c) full protein including disordered regions; and (b) and (d) only structured part.

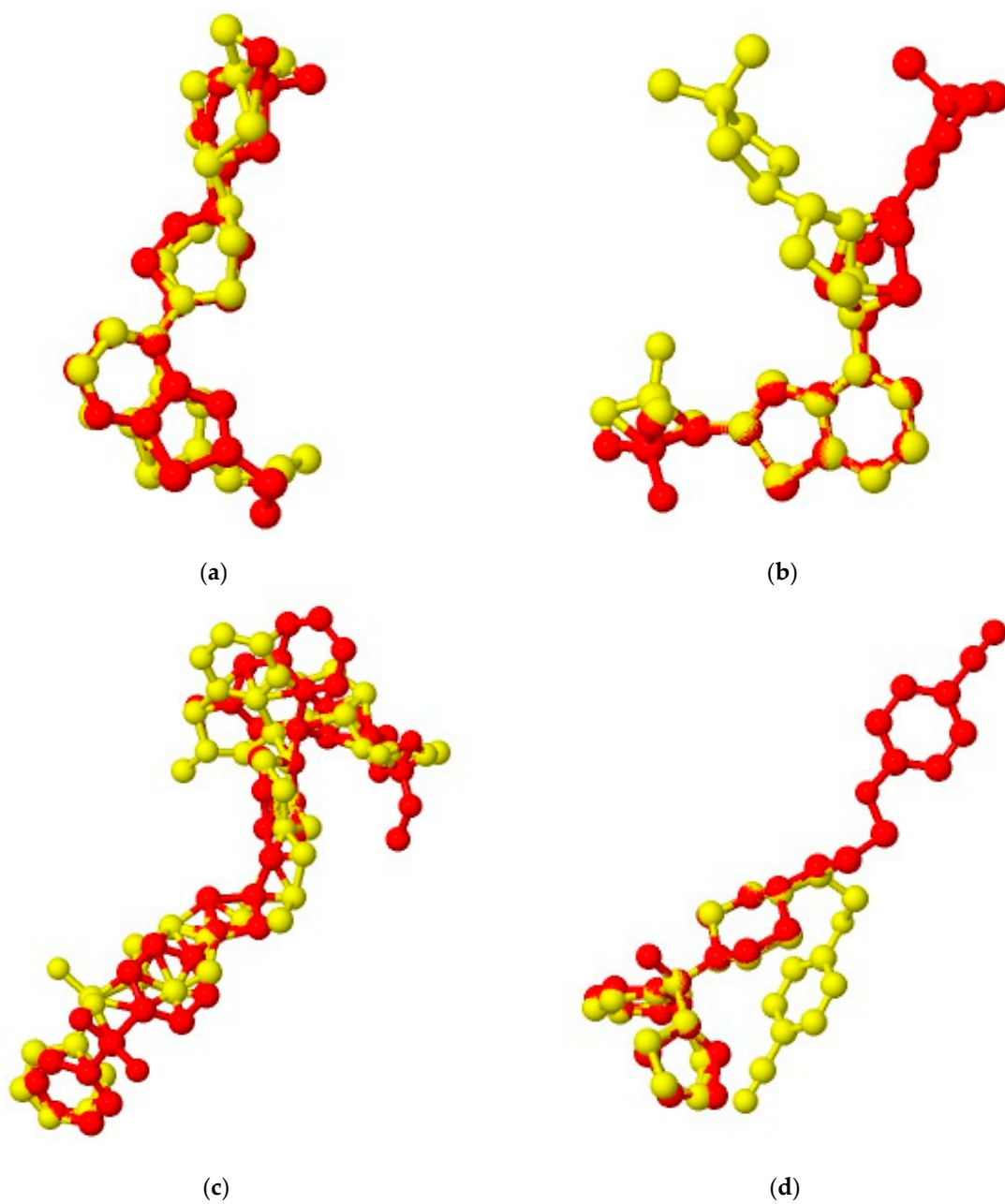
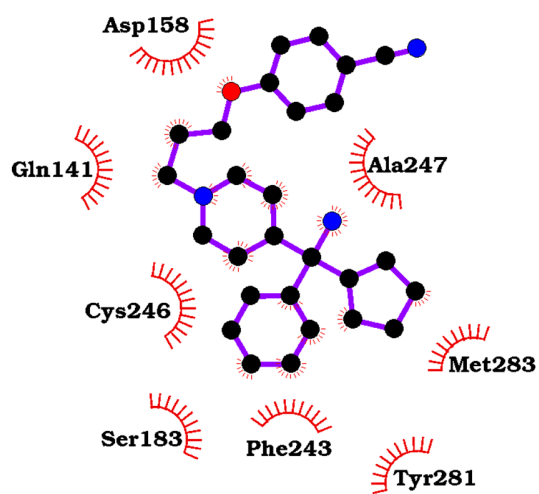
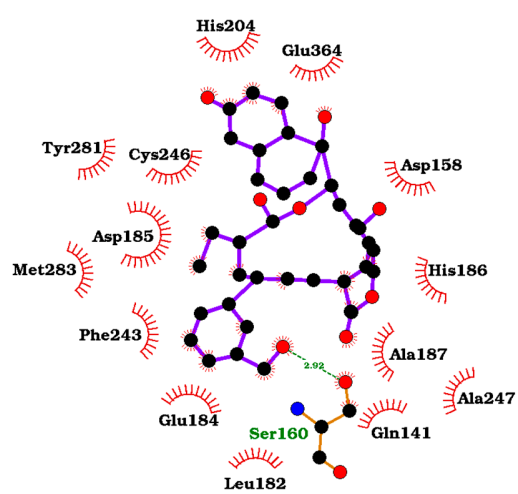


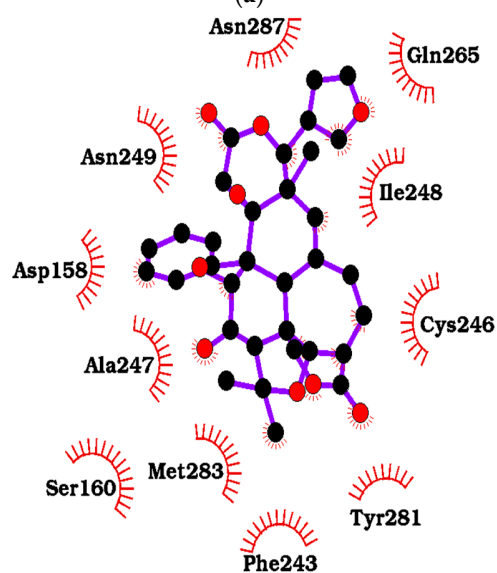
Figure S3. Superimposition of the best pose from AutoDock Vina docking to the co-crystallized structures for (a) MI-2 (0RO), (b) MI-2-2 (0RT), (c) MI-89, and (d) MIV-6. For all the superimpositions, the co-crystallized ligands are in red while the docking poses are coloured yellow.



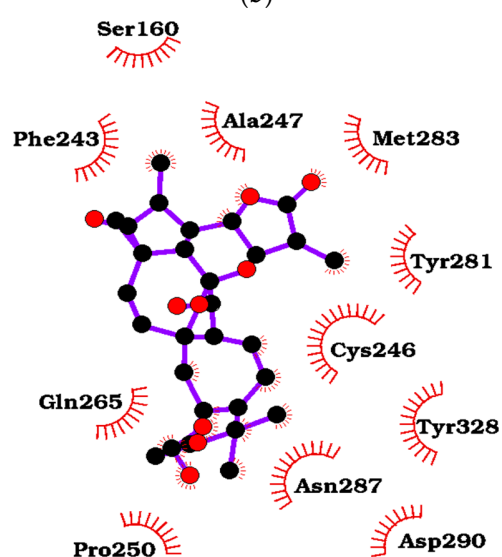
(a)



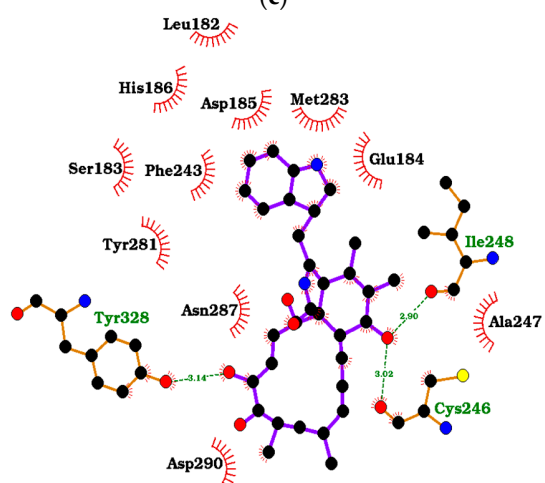
(b)



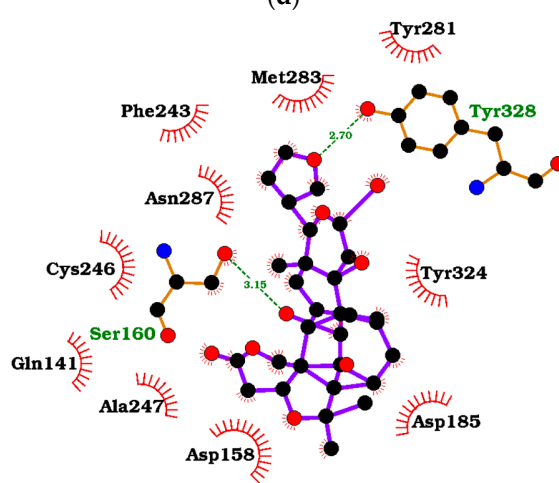
(c)



(d)



(e)



(f)

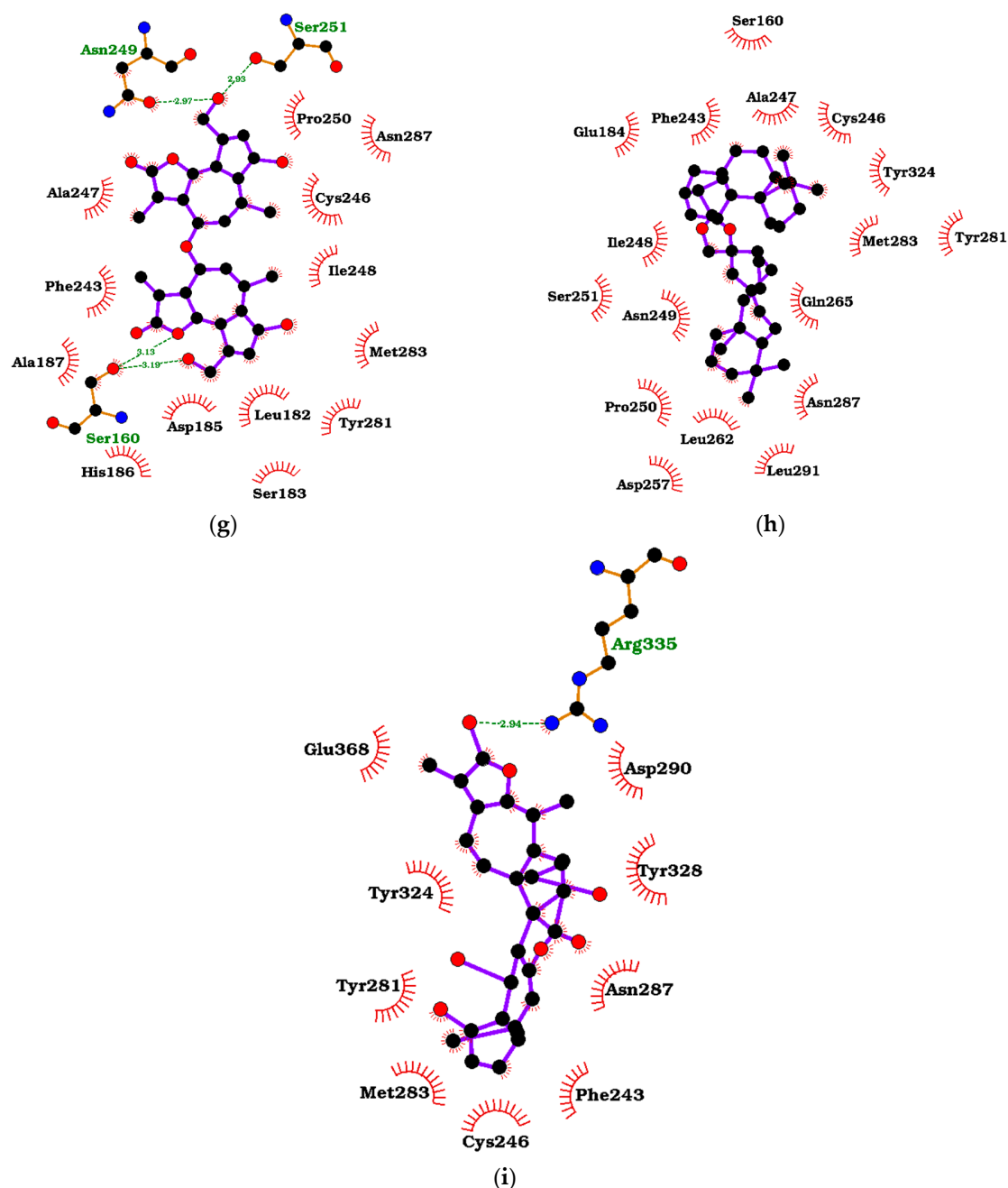
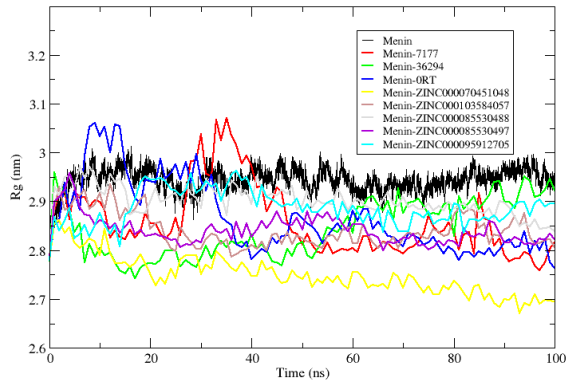


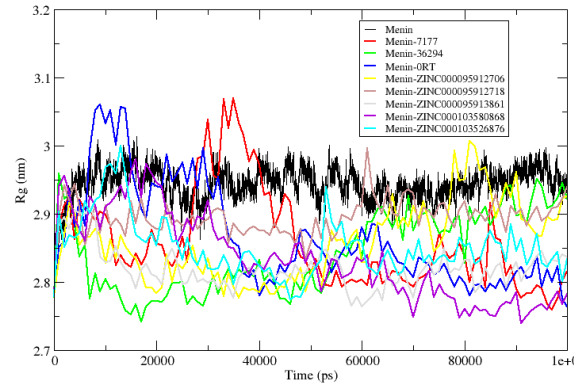
Figure S4. Protein-ligand interaction maps of menin in complex with (a) CID 71777742, (b) ZINC000103526876, (c) ZINC000085530497, (d) ZINC000095912718, (e) ZINC000070451048, (f) ZINC000085530488, (g) ZINC000095912706, (h) ZINC000103580868, and (i) ZINC000103584057.

Radius of gyration (total and around axes)



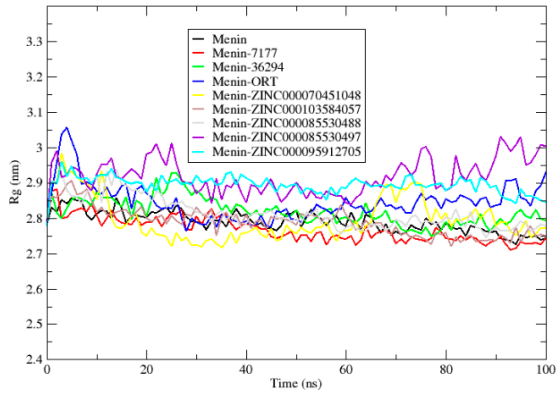
(a)

Radius of gyration (total and around axes)



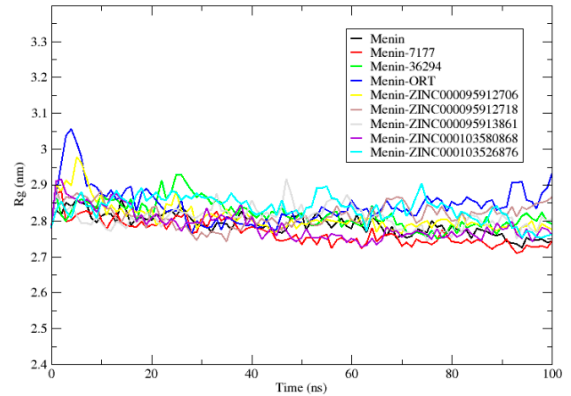
(b)

Radius of Gyration (MD Run 2: Full Protein)



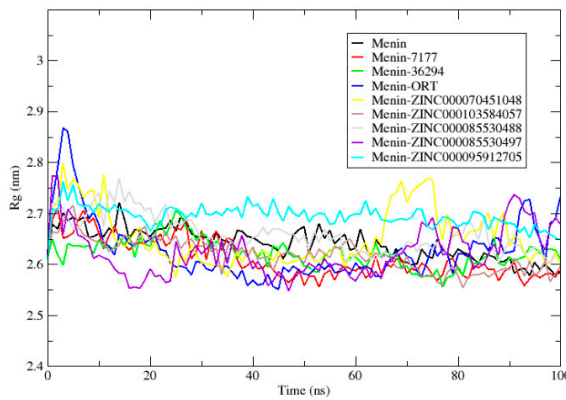
(c)

Radius of Gyration (MD Run 2: Full Protein)



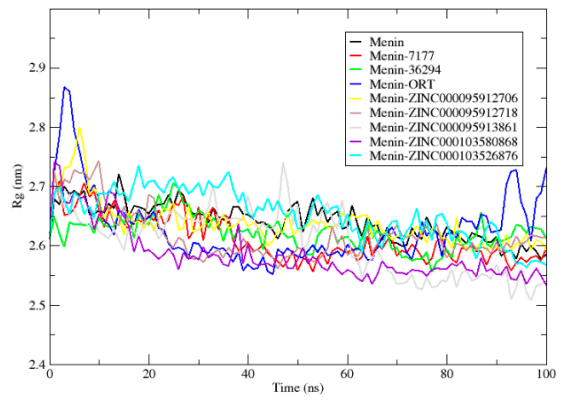
(d)

Radius of Gyration (MD Run 2: Only Ordered Part)



(e)

Radius of Gyration (MD Run 2: Only Ordered Part)



(f)

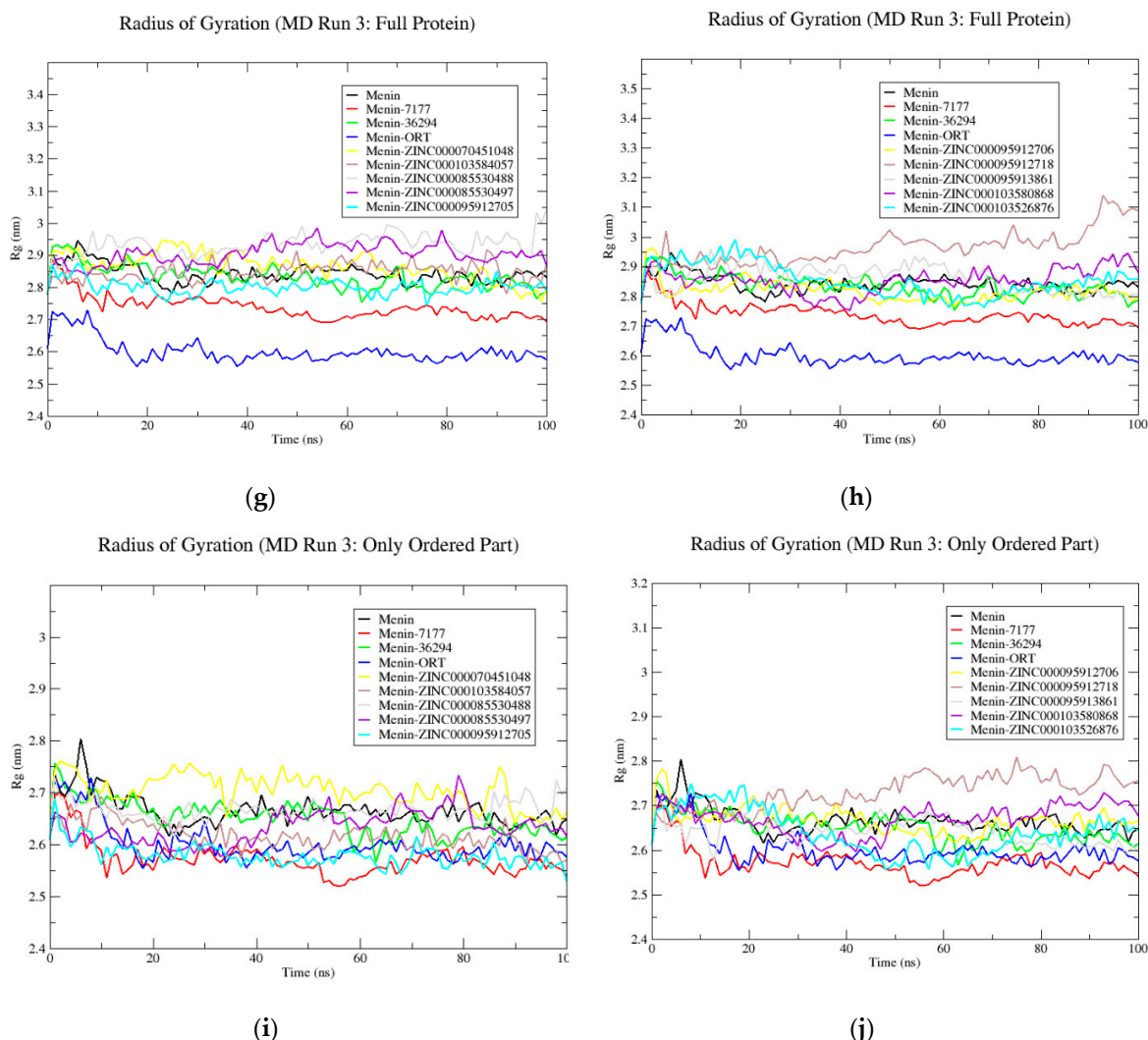
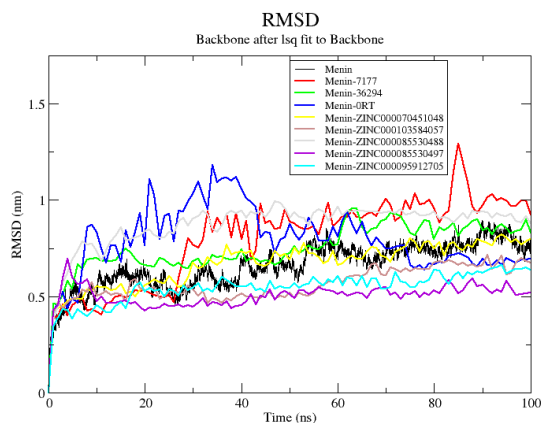
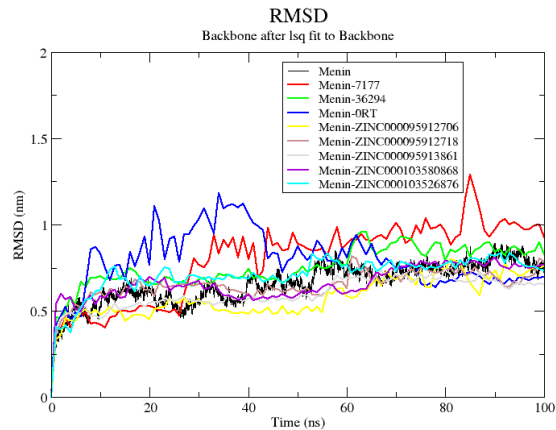


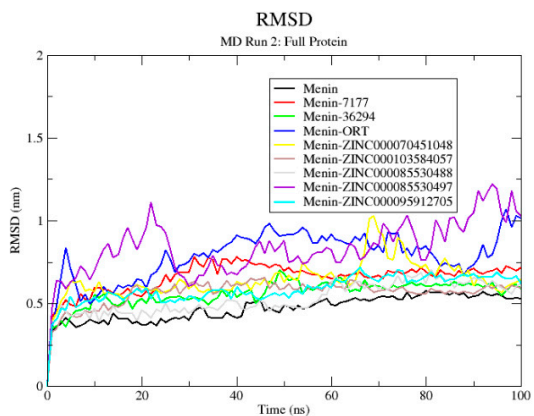
Figure S5. Radius of gyration plots of only the structured region of the unbound menin protein and the menin-ligand complexes generated using GROMACS after 100 ns simulation. The Rg plots were generated using: (a) and (b) whole menin structure from MD run 1; (c) and (d) whole menin structure from MD run 2; (e) and (f) only structured regions of menin from MD run 2; (g) and (h) whole menin structure from MD run 3; and (i) and (j) only structured regions of menin from MD run 3. The unbound protein is coloured black while the known inhibitors CID 71777742, CID 36294 and 0RT are coloured red, green, and blue, respectively.



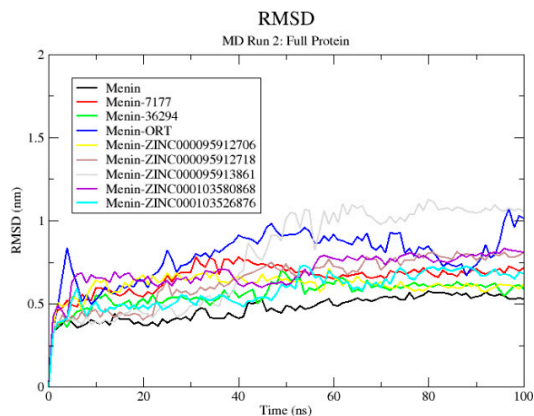
(a)



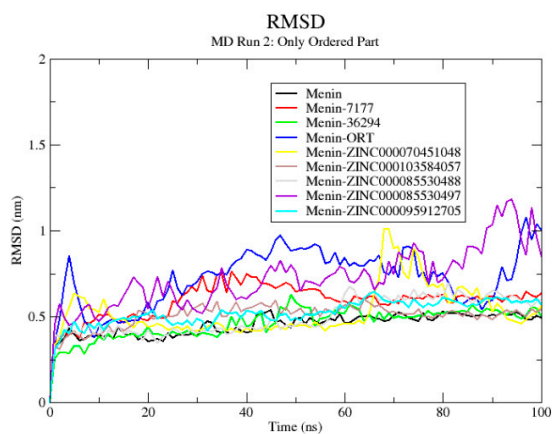
(b)



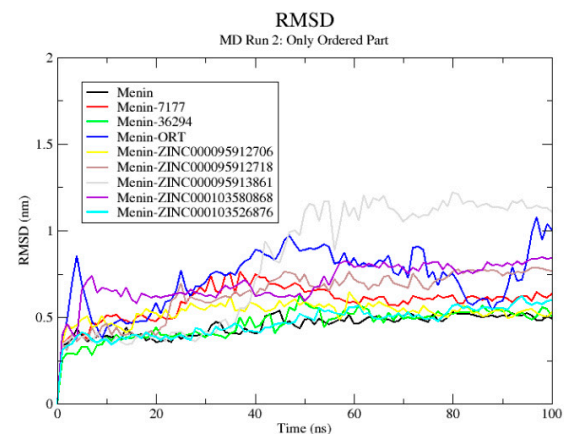
(c)



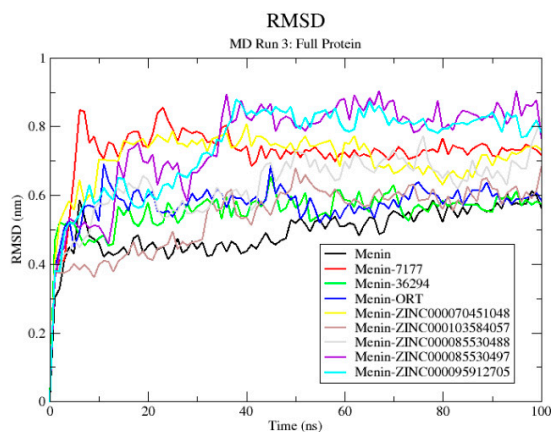
(d)



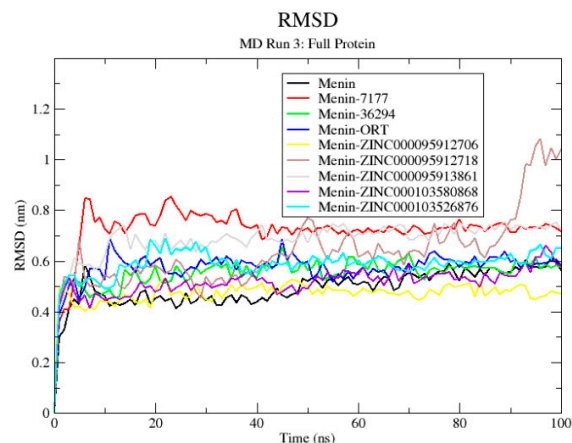
(e)



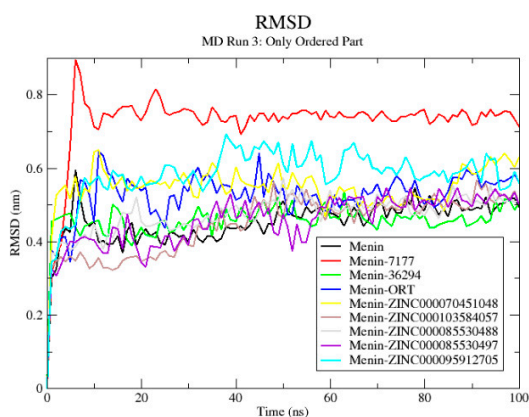
(f)



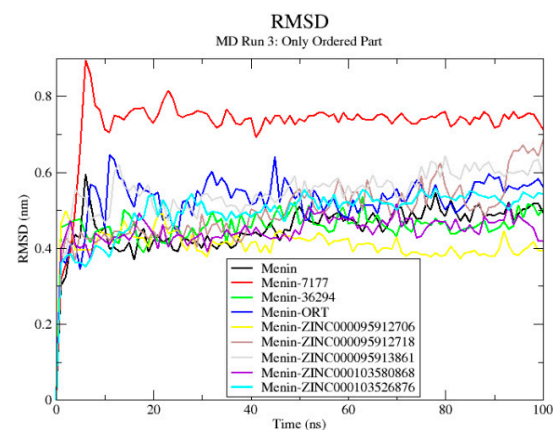
(g)



(h)



(i)



(j)

Figure S6. Root mean square deviation of the unbound menin protein and the menin-ligand complexes generated using GROMACS after 100 ns simulation. The RMSD plots were generated using: (a) and (b) whole menin structure from MD run 1; (c) and (d) whole menin structure from MD run 2; (e) and (f) only structured regions of menin from MD run 2; (g) and (h) whole menin structure from MD run 3; and (i) and (j) only structured regions of menin from MD run 3. The unbound protein is coloured black while the known inhibitors CID 71777742, CID 36294, and ORT are coloured red, green and blue, respectively.

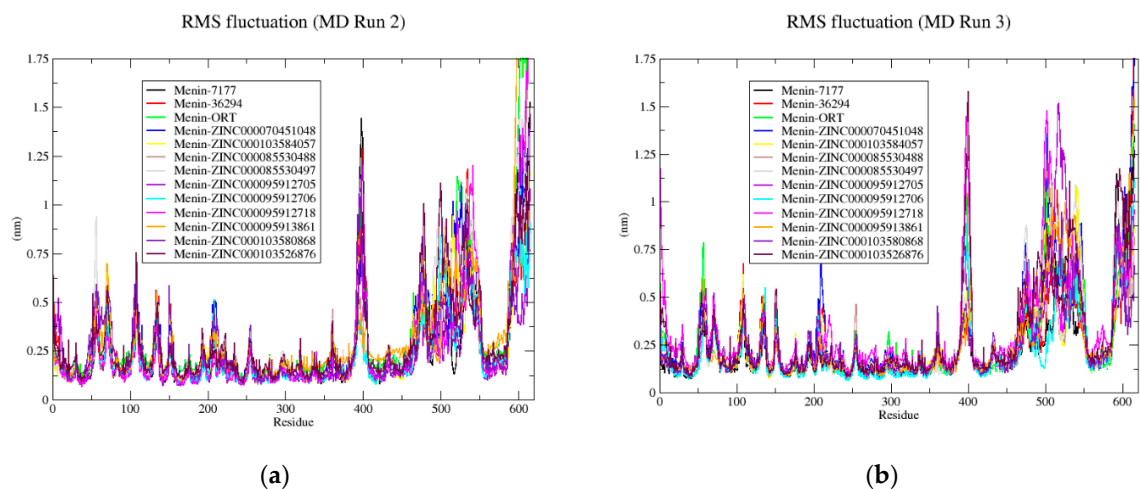
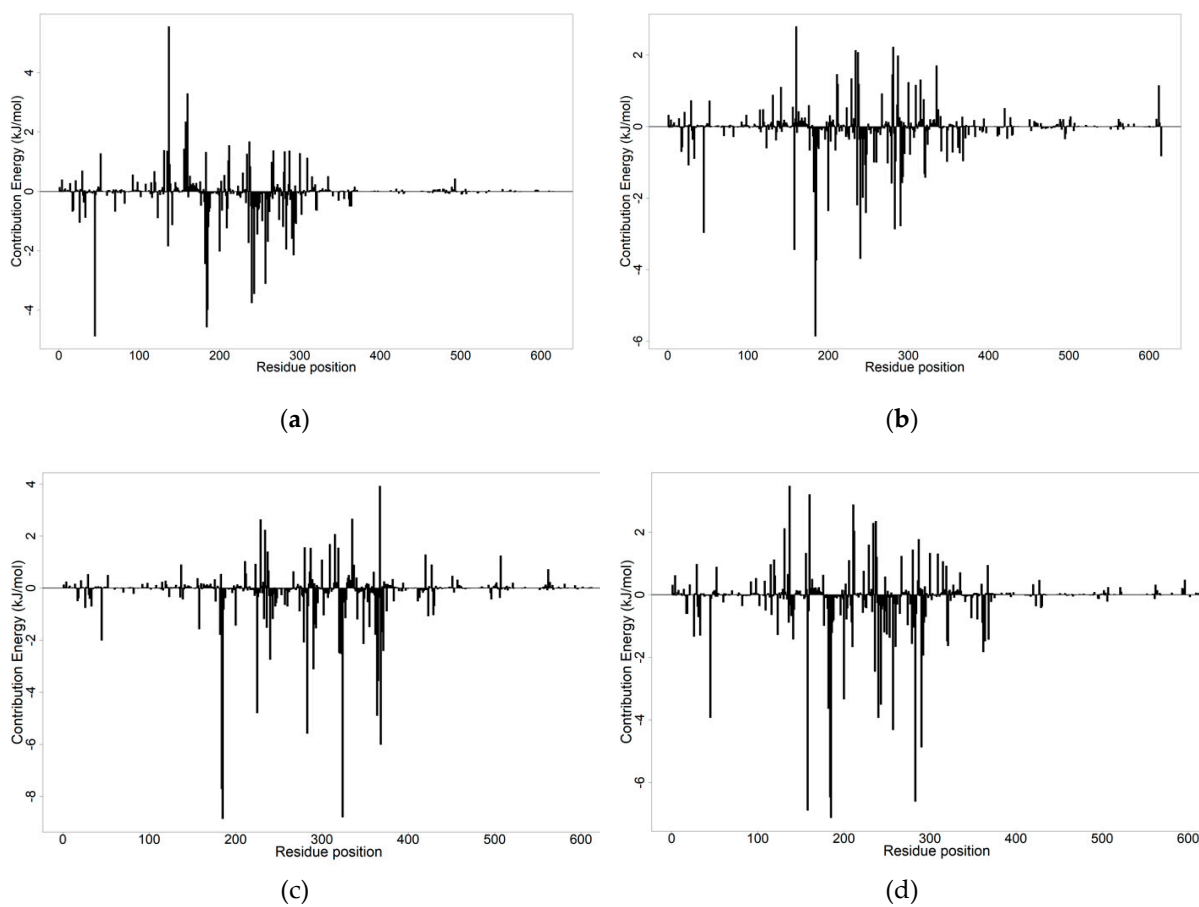
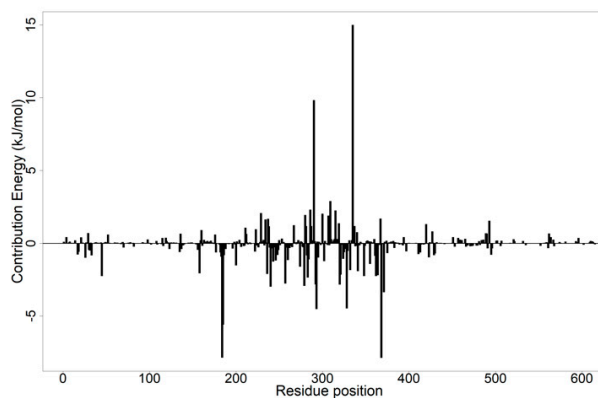
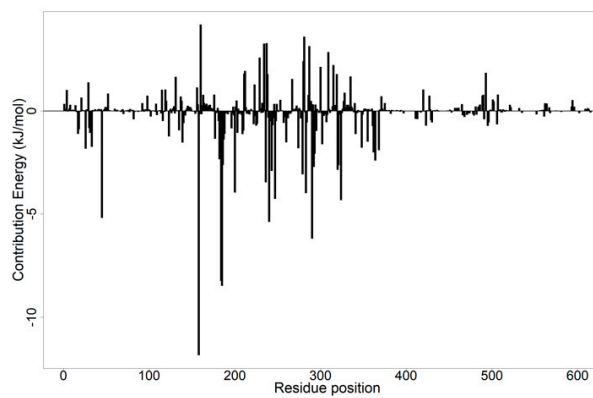


Figure S7. Root mean square fluctuation plots for menin-ligand complexes generated using GROMACS after 100 ns simulation for (a) MD run 2 and (b) MD run 3. The known inhibitors CID 7177742, CID 36294 and ORT are coloured as purple, red, and green, respectively.

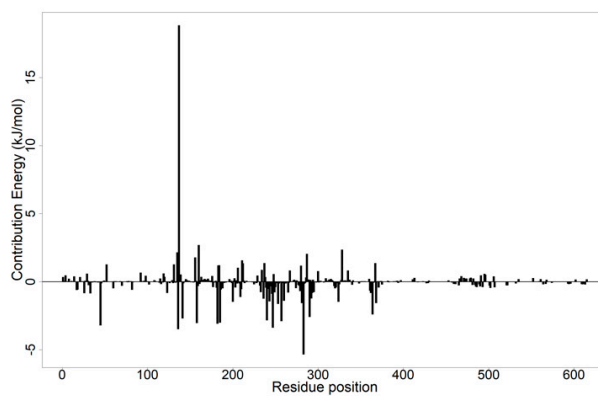




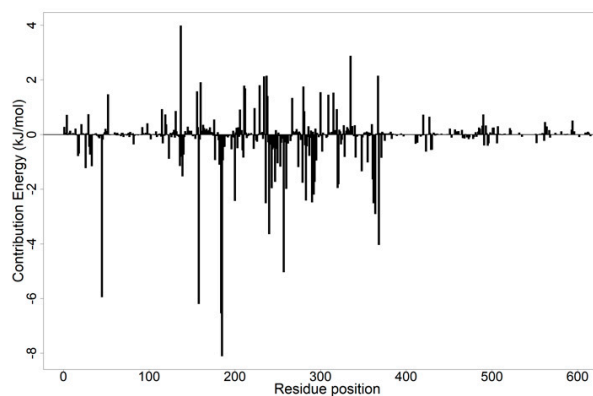
(e)



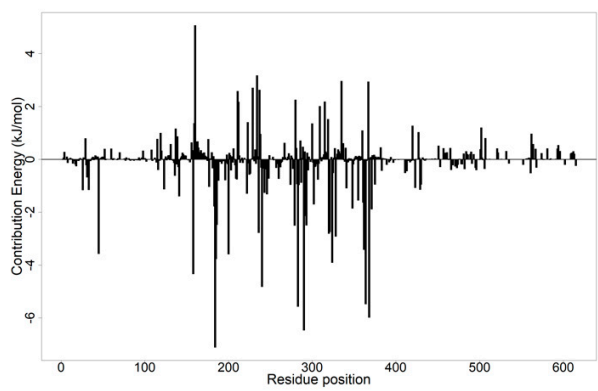
(f)



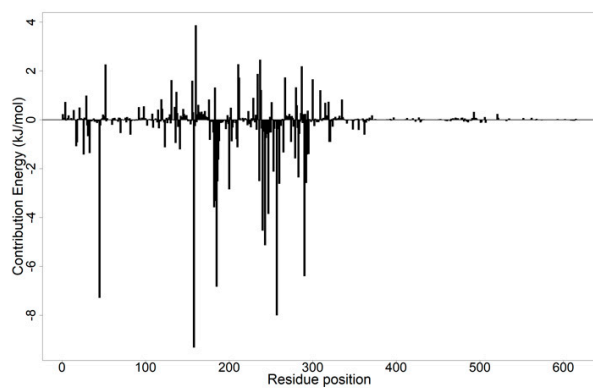
(g)



(h)



(i)



(j)

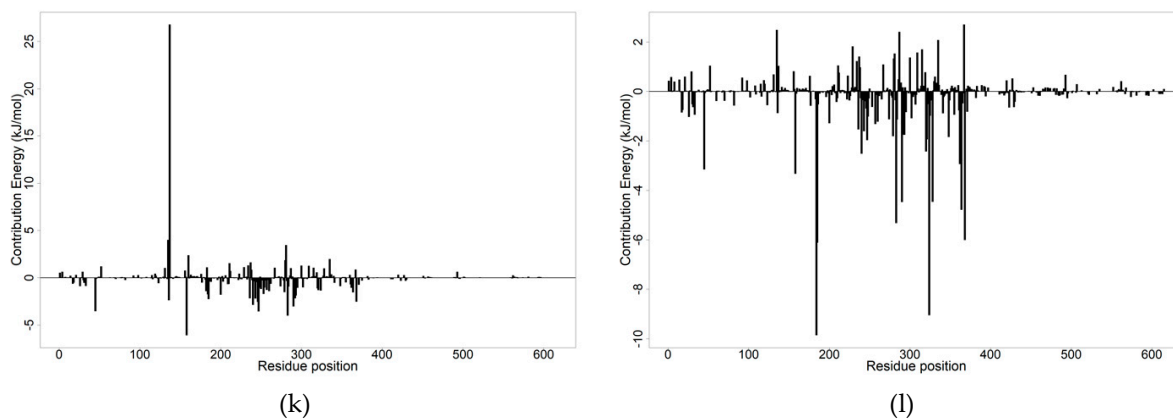


Figure S8. Per-residue energy decomposition of the menin-ligand complexes: (a) 0RT, (b) 36294, (c) 71777742, (d) ZINC000095912705, (e) ZINC000103526876, (f) ZINC000085530497, (g) ZINC000095912718, (h) ZINC000070451048, (i) ZINC000085530488, (j) ZINC000095912706, (k) ZINC000103580868, and (l) ZINC000103584057.